ECOspec: Microplastic Identification with Raman Spectroscopy

Sophia Adams[1], Michael Rusinko[1,2], Landon Morjal[2], and Logan Sullivan[2]

[1]CREOL, University of Central Florida, Orlando, Florida, 32816-2450

[2]Dept. Of Electrical Engineering and Computer Engineering, University of Central Florida, Orlando, Florida, 32816-2450

***Abstract* — Microplastics in water have become a growing environmental concern, and current detection methods are often time-consuming or require complex equipment. This project introduces ECOspec, a compact system that uses Raman spectroscopy to detect microplastics in water samples. By using a 785 nm laser, optical filters, and a spectrometer, the system captures unique spectral signatures that can be used to determine different types of plastics. ECOspec combines optical, electrical, and software components into a portable setup that allows for non-destructive and real-time analysis. The results show that a smaller, more accessible solution for monitoring water quality is both practical and effective.**

***Index Terms* — Czerny-turner spectrometer, Microplastics, Raman Spectroscopy, Spectral Analysis, Water Monitoring**

I. Introduction

Microplastic pollution has become an increasingly widespread issue due to the rapid growth in global plastic production and waste. These particles, typically smaller than five millimeters, have been detected in oceans, freshwater systems, and even drinking water, raising concerns about their impact on environmental and human health. Due to their persistence, reliable detection and identification methods are critical for effective environmental monitoring and long-term risk assessment.

Traditional techniques for identifying microplastics, such as visual inspection, density separation, and basic physical testing, are often time-consuming, subjective, and in some cases destructive to the sample. These methods cannot accurately distinguish between different polymer types, which is essential for understanding sources and environmental impact. As a result, optical spectroscopy techniques have gained attention to their ability to provide rapid and material-specific analysis. Raman spectroscopy enables non-destructive identification by measuring the inelastic scattering of light, producing a unique spectral fingerprint corresponding to the molecular structure of a material.

This project presents ECOspec, a compact Raman spectroscopy system designed for microplastic detection in water samples. The system utilizes a 785 nm diode laser as the excitation source, selected to minimize fluorescence interference while maintaining sufficient signal strength.

The system incorporates two different processing units for data acquisition and control system components. The spectrometer output is digitized and processed through software that performs baseline correction, noise reduction, and peak detection. The processed spectra is compared against a reference database of known polymer signatures to classify the sample. This integration of optical sensing and embedded processing enables near real-time identification of microplastics.

ECOspec aims to detect and identify microplastics in water using Raman spectroscopy by capturing characteristic spectral fingerprints of polyethylene terephthalate, polystyrene, and nylon. Our engineering specifications that are demonstratable include the identification accuracy, >70%, detection in a reasonable time frame, <60 seconds, and it will have a minimum detectable concentration, which is still being evaluated through testing. By combining optical, electronic, and software subsystems into a single platform, ECOspec aims to provide a practical solution that can be deployed outside of traditional laboratory environments.

II. Background

A. Raman Spectroscopy

Raman spectroscopy is a material identification technique based on elastic and inelastic light scattering. Rayleigh scattering dominates and preserves photon energy, while Raman scattering (~10^{-8} probability) produces frequency-shifted photons characteristic of molecular vibrational modes. Scattering efficiency is governed by the Rayleigh cross section, with intensity proportional to λ^{-4}. In Raman systems, the excitation beam is tightly focused to maximize power density, enhancing Raman signal generation and spatial specificity for accurate spectral identification.

B. Why use Raman for Microplastic Analysis

Plastic molecules are organic molecules made of chains of hydrocarbons, with unique geometries and energy levels. These differences produce Raman peaks at certain wavenumbers, providing the molecule with its own Raman fingerprint. This high chemical specificality enables differentiation between polymers with very similar

compositions. From polyethylene terephthalate (PET), Fig. 1, in water bottles to expanded polystyrene (EPS) in styrofoam, Fig. 2, the plastics commonly used in modern day each have unique Raman spectra.

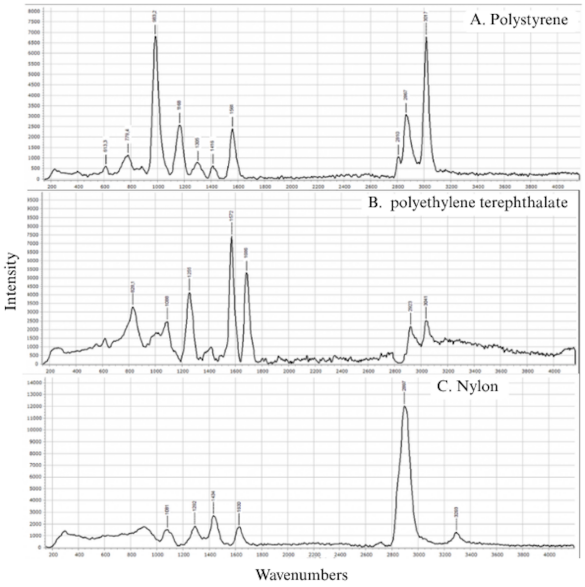

Fig. 1. A: Raman spectra of polystyrene, with key peaks at 983, 1561, 2867, and 3017 wavenumbers. B: Raman spectra of polyethylene terephthalate, with key peaks at 828, 1255, 1572, and 1666 wavenumbers. C: Raman spectra of nylon, with notable peaks at 1434, 2697, and 3293 wavenumbers.

Additionally, Raman spectroscopy is well-suited for microplastic analysis because it is non-destructive in nature and requires minimal sample preparation, allowing samples to be analyzed without altering or damaging their structure. Water also has a weak Raman signal, making Raman spectroscopy a useful tool for samples in aqueous environments.

III. Optical Hardware Overview

ECOspec uses a 785 nm laser excitation source, beam conditioning optics, and an infinity-corrected microscope objective to illuminate and collect Raman signal from samples. The collected light is filtered and imaged through a tube lens onto a slit, then dispersed using a crossed Czerny-Turner spectrometer.

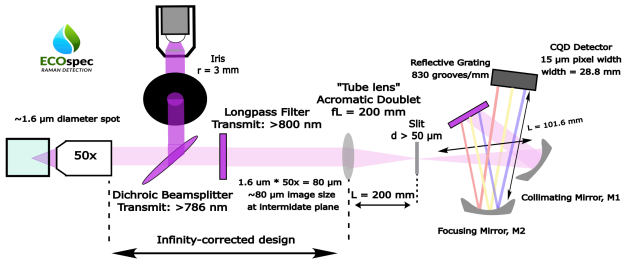

Fig. 2. Optical hardware diagram, illustrating the excitation laser, the sample, the probe optics, filtering, and spectrometer.

IV. Probe Optics

A. Laser and Fiber-collimator

Our laser of choice is the 785 nm Ocean Optics Raman Laser. It boasts a 0.2 nm linewidth with adjustable optical output power up to 350 mW continuous wave. The narrow linewidth is necessary to resolve our desired Raman spectra. This is a standalone device that offers remote power control and remote laser shut off. The laser module is SMA connector coupled, allowing for fibers with SMA ports to be attached. A metal-coated fiber will be used to direct the output of the laser into the system while ensuring minimal power loss and user exposure to potentially high-power infrared light.

B. Infinity Corrected Objective System

To maximize collection of Raman scattering, a high NA microscope objective must be used in conjunction with an input laser beam that minimizes the spot size to micron levels. Our microscope objective of choice is the 50x Nikon CF160 TU ELWD infinity-corrected Brightfield microscope objective. The infinite conjugate correction is critical in our design for two reasons: our input laser beam is collimated, and our collection optics must be as dense as possible. The infinite conjugate enables us to reduce component count, minimize laser beam spot size, and use an achromat lens to focus light into the spectrometer instead of Nikon's 200mm tube lens. Using (), this objective produces a spot size of 1.6 micron however a spot size of ~2 micron will likely be reached.

C. Dichroic Mirror

A 785 nm "RazorEdge" long-pass edge filter is selected as the reflecting surface for the laser. This dichroic mirror allows for the laser to excite the sample while allowing a majority of the Raman scattering to pass through. This is common practice in many micro-Raman setups.

D. Extra Filtering

While the dichroic mirror isolates a majority of the 785 nm laser light from the detector, some light is still able to get through. To reduce this intensity, an 805 nm> cut on dichroic filter nm is used to further isolate the spectra. Some Raman scattering is cut off, but they are not in our range of interest.

E. Cage System

To ensure our optics are aligned during transport and protected from user error, an optical cage system is used to maintain alignment of the probe system's optical components.

V. Spectrometer Design

A. Spectrometer Design Specifications

The spectrometer disperses the filtered Raman signal onto a detector for wavelength-resolved measurement. The design begins by identifying a few key parameters, such as the ideal spectral range of the detector. For our plastics of interest, polyethylene terephthalate, polystyrene, and nylon, their fingerprint Raman peaks occur between 0 – 3200 wavenumbers. As shown in (2), the conversion between Raman shift is dependent on the laser wavelength, 785 nm, and the intensity of the Raman scattering. Therefore, our spectral range for our spectrometer is 780 – 1050 nm based on (2), with a center wavelength of 915 nm.

$$\Delta\upsilon\ (cm)\text{^}(-1) = \ |1/\lambda\_laser\ - 1/\lambda\_Scattering\ | \cdot 10\text{^}(-7) \qquad (1)$$

Design constraints include a fixed detector with a width of 28.8 mm and a spectrometer configuration. A Czerny–Turner layout was selected due to its widespread use and high-resolution capability. After alignment challenges with the M-type geometry, a crossed Czerny–Turner design was adopted for improved alignment and detector integration. Ray tracing confirmed that the crossed configuration meets compact system size requirements.

B. Slit Size

The slit width of our spectrometer determines the resolution of our system. A narrow slit directly correlates with a higher resolution- it defines the initial beam width that disperses, and a narrow slit will produce a smaller image on our detector plane, indicating a higher resolution. But that can also limit our signal, so the tradeoff between resolution and signal is key- especially for Raman spectroscopy and its signature low signal. To balance those tradeoffs, it is good practice to optimize the light entering your spectrometer by matching the image size from your focusing optic to the width of your slit or make it slightly smaller. After the diffracted limited spot size from the output of the microscope objective was calculated earlier, resulting in 2 μm, that spot size can be used to find the resultant image size at the focal point of the tube. The equation below for the image size resulted in a 80 μm image size based on the magnification of the objective and tube lens system, Therefore, a slit that is 60 μm - 100 μm should be selected, to match the image size as much as possible. Currently, we are testing with a 100 μm slit to improve our resolution. Once the light enters the slit, it hits mirror one, which is the collimating mirror. It then projects the collimated signal onto a diffraction grating, which splits the signal into its separate wavelengths, and is then reflected onto a focusing mirror which focuses each split-up wavelength onto a certain pixel on the detector.

C. Collimating and Focusing Mirrors

The collimating and focusing mirrors that were donated for our senior design project are a circular, spherical gold coated collimating mirror, and a rectangular, spherical gold focusing mirror, both with a local length of 102.6 mm, from Torrent Photonics. The focal lengths defined the distance from the slit to the collimating mirror, and the length from the mirror to the detector, before optimization. The gold coating maximizes the mirrors power in the NIR.

D. Grating

The grating choice is vital for defining the range and resolution of our Raman spectrometer. This separation allows us to discern each Raman shift that corresponds to the vibrational mode, which is used for identification and detection of plastics. This separation is done by the optical properties of the diffraction grating, and is dependent on the angle of incidence, shown in (2). λ is our central wavelength, at 920 nm, d is our groove size, calculated to be 1.2048 μm. We can start with a symmetric design, with our incidence angle, α, equal to our diffracted angle, β. After (2), our working angles come out to be 22.5 degrees.

$$m\lambda = d(\sin(\alpha) + \sin(\beta)) \qquad (2)$$

Dispersion can be approximated using (3), based off the central wavelength, grating groove size, and the angle of diffraction- resulting in a dispersion of approximately 0.0923 mm/nm.

$$d\beta/d\lambda = 1/(d \cdot \cos(\beta)) \qquad (3)$$

E. Detector and Resolution

Dispersion is key for determining the pixel resolution, and our detector. This is an important parameter for defining resolution, because our pixel resolution is dependent on the pixel size and approximate dispersion, seen by (4), resulting in a calculated pixel resolution of 0.16 nm/pixel. Our real resolution will be determined by our slit size, most likely 0.2-0.4 nm, corresponding to Raman shift resolution of 5-10 wavenumbers depending on the wavelength.

$$d\lambda = (Pixel\ Size)/(d\beta/d\lambda \cdot .90) \quad (4)$$

We also verified that the dispersed light after the grating will fit onto our detector with a width of 28.8 mm. Based on the wavelength span per mm, an inverse of the dispersion, the calculated wavelengths expected at the left and right edge of the detector face correspond to 764 and 1076 nm- fitting right into our spectral range.

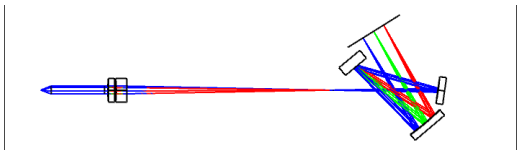

Fig. 3. First-order ray trace of collection optics, starting at the sample scattering on the left.

VI. Electrical Hardware

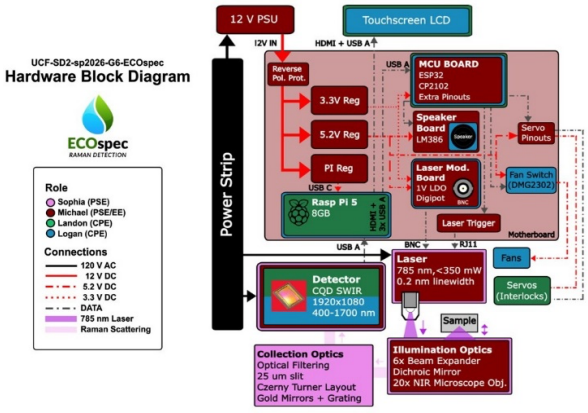

Fig. 4. Hardware Block Diagram

A. Detector

A colloidal quantum dot (CQD) short-wave infrared (SWIR) from onsemi's ACUROS model cameras is the detector of choice for this system. The CQD sensor has a responsivity range of 400-1700 nm, with a quantum efficiency of ~28% in our wavelengths of interest. The camera module also has a dynamic range of 70 dB with an internal TEC that allows cooling down to 15 °C.

However, for the TEC to operate at low temperatures, thermal management must be introduced. Copper heatsinks, aluminum heatsinks, and fans are strategically placed around the camera to force hot air away from the system. Lowering the temperature of the TEC also requires us to produce a new non-uniformity correction (NUC) table to compensate for heated and dead pixels. This is done by taking a flat-white and complete dark image with the camera for the software to correct with.

B. Control and Safety Systems

Laser control and safety is implemented using a dedicated ESP32 dual core microcontroller. This device is intentionally isolated from the primary processing unit to ensure that all safety functions remain independent of software execution on the processing system, maintaining a failsafe design, preventing unintentional laser operation.

The ESP32 controls the laser's external shut-off circuitry, which is configured in such a way that any open circuit forces the laser to enter a disabled state.

The laser's power is externally controlled via BNC. A DC voltage between 0 – 1 V controls the output power from 0-100%. This control voltage is generated by the AP7366EA 1 V LDO and then modulated by the TPL0501 digital potentiometer. This enables slow but fine adjustment of CW output power. The TPL0501 has 256 positions for the wiper resistor and communicates via SPI.

A speaker board enables the MCU to indicate to the user what type of state the system is in.

Communication between the ESP32 and the Raspberry Pi is handled over a UART serial communication. This enables the exchange of control commands. However, laser conditions are strictly governed by the logic on the ESP32 and do not rely on continuous communication from the Raspberry Pi. This strict separation means that loss of communication or system errors will not result in unsafe laser operation, providing assured safety.

C. Processing and Interface Hardware

The processing hardware is built around a Raspberry Pi 5 equipped with 8 GB of LPDDR4X memory, selected for its high-performance embedded computing capabilities and extensive peripheral support. The platform is based on the Broadcom BCM2712 quad-core Cortex-A76 processor operating at up to 2.4 GHz, providing sufficient

computational headroom for sustained data acquisition and system control tasks. The Raspberry Pi serves as the central hardware controller, interfacing directly with the CQD SWIR detector over a USB 3.0 connection, which enables high-bandwidth transfer of full-frame spectral data with minimal latency. A dedicated HDMI interface connects the Raspberry Pi to a touchscreen display, enabling standalone system operation without external computing hardware.

D. Power Systems

ECOspec uses very sensitive and precise equipment. Thus, proper power systems and protections must be put in place to prevent any sort of electrical damage to the overall system. The camera module and laser are precise and delicate standalone devices. These larger components are powered with their dedicated OEM PSUs. The MCU, peripheral boards, Raspberry Pi, cooling system, and safety interlocks are powered by a 12 V DC COTS 5.5x2.5 mm barrel jack PSU, where power is distributed via the motherboard. The motherboard also includes access to 12 V screw terminals which draw directly from the COTS PSU in the case of upgrades such as 12 V fans or a Peltier cooler are desired.

Various power protection circuits are implemented on the motherboard. The motherboard contains multiple switches which control output for debugging, optional power ports, and a “DEV Mode” for use of a generic ESP32 Devkit V1. At the barrel jack input, a Schottky diode with a low reverse voltage and a TVS diode with a clamping voltage at 16.4 V are put in place in the case of a reverse polarity, ESD, or power surge event. The 12 V screw terminals and each voltage regulator has a dedicated PMOS FET for reverse voltage protection. The 5 V fan output screw terminals have flyback diodes to minimize any back EMI generated when shut off.

The voltage regulator boards were designed around the TI LM2679 ADJ switching regulator. It accepts 8-40 V input and outputs 1.23-37 V depending on the feedback resistor values, and is rated for a 5 A output (7 A max). ECOspec requires dedicated voltage supplies: 3.3V 2A for the MCU board and peripherals, 5.2 V 3 A for the fans, servos, and peripherals, and a dedicated 5.2 V 5 A for the Raspberry Pi 5 to operate in high power mode. Each of these regulators also have their own dedicated Schottky and TVS diodes in the event of an electrical incident.

VII. Software

A. User Interface

The user interface was developed as a native touchscreen application running on a Raspberry Pi 5 with a 1024×600 display. It is built using HTML5, CSS3, and JavaScript, and rendered through PyWebView with a GTK backend. Communication between the interface and the Python-based hardware and processing system is handled using the PyWebView JavaScript bridge. The interface is organized into four fixed sections that are all visible at once, eliminating the need for navigation between screens. A header bar displays the real-time connection status of the Raspberry Pi 5, ESP32 microcontroller, ACUROS CQD camera, and 785 nm laser. These statuses are automatically updated every five seconds. The spectrum panel displays the processed Raman spectrum using an HTML5 canvas and updates in real time during data acquisition. Once a scan is complete, the identification panel shows the most likely material match, along with its Pearson similarity score and the next two closest matches from the reference library. The acquisition settings panel allows the user to start a scan or trigger an emergency stop if needed. A real-time system log records hardware activity, scan progress, and any errors with timestamps for traceability. For data handling, processed spectra can be exported as CSV files to a user-selected location. To ensure safe operation, the scan button remains disabled until both the ESP32 and camera are confirmed to be connected, preventing scans from being initiated without the required dependencies being initiated and ready for acquisition.

Fig. 4. ECOspec user interface displaying real-time Raman spectrum acquisition, system status, and results.

B. Data Processing

To perform material identification, robust data processing pipelines are required. This pipeline is implemented in the Python programming language. Python was selected for its extensive scientific computing ecosystem, making it optimal for performing advanced transformations on the large datasets produced from a spectral acquisition. The data processing pipeline begins with the initial cleaning step of an acquired raw spectra from a CSV file, where invalid readings are removed. The spectral range will also be restricted to 200-3400cm^{-1}.

The dataset is then interpolated across a fixed $1cm^{-1}$ wavenumber grid. Without this step, other operations downstream would produce useless outputs or fail due to requiring a clean indexing of values.

After indexing, an initial median filter is performed with a kernel of size 15 to remove many instances of random noise produced by sources such as cosmic ray interference.

Another common cause of interference in Raman spectroscopy that requires addressing at a processing level is the introduction of a broad fluorescence background, which presents a broad baseline shift. To remove this, a polynomial fit is performed. This technique is done using a seventh-degree polynomial but can be configured programmatically to better fit other applications. This step allows further isolation of Raman peaks to make identification easier.

Processing steps upstream from this point have all been focused on ensuring the data shape is preserved. After these are completed, now the data must be adjusted to account for major intensity differences or scaling effects. To remove misleading information presented from this effect, a Standard Normal Variate normalization is performed, which centers the data to a mean of zero, and scales the standard deviation to one. Completion of this step allows for the spectra to be comparable independent of the magnitude.

The final step of data transformation is a final scaling step to ensure all data is within a consistent range, eliminating the possibility of extreme value from dominating our comparison metrics. This goal is achieved through implementation of Min-Max scaling, which simply scales the processed data between [0-1]. After this, acquired spectral data can be utilized for comparison and identification.

After preprocessing, spectra are compared to a reference library processed using the same pipeline to ensure consistency and reduce false positives. The processed spectrum is saved as a CSV and passed to the identification stage, where similarity to known, materials is evaluated using the Pearson correlation coefficient. This approach enables robust material discrimination based on spectral shape, even in the presence of noise and baseline distortion.

C. System Control Firmware

System control responsibilities are split between the ESP32 and Raspberry Pi units, with a constant line of communication between the two. The Raspberry Pi unit serves to host the user interface, which utilizes multiple application specific libraries to offer responsive and robust control of the overall system. The Pi also handles tasks requiring a higher level of computing, such as data processing and control of the camera unit. For peripheral controls, such as chamber locks, laser control, etc., the Raspberry Pi issues commands to the ESP32 via UART.

UART enables seamless communication between the two control units. The ESP32 utilizes FreeRTOS, enabling the controller to receive and respond to issued commands in a deterministic manner. This architecture ensures bounded response times for safety-critical operations such as emergency system shutdown. Determinism is required due to the increased safety risk of an unsecured laser. Within the FreeRTOS task structure, the additional duties of the ESP32 are distributed.

This task structure allows the ESP32 to take control of multiple peripherals as required. For ECOspec, it handles locking of the chamber doors utilizing PWM signals to control the angle of servo motors. Additionally, it uses GPIO control pins to allow functionality such as lasers to enable signals, emergency shut offs, and cooling fan control. With the use of a small, lightweight filesystem, such as the Serial Peripheral Interface Flash File System (SPIFFS), the ESP32 is able to store audio files and perform playback when a user needs to be notified. Output of the audio is handled by the Inter-IC Sound (I2S) interface. This protocol allows for playback utilizing a Digital-to-Analog Converter (DAC), by sampling the audio file itself, and outputting a corresponding audio signal.

The final peripheral controlled by the ESP32 is the laser modulation board. This board is controlled by a digital potentiometer, which interfaces via Serial Peripheral Interface (SPI) to the microcontroller. The TPL0501 is a write only device. Control of this peripheral is performed through SPI transactions on the bus, which writes to an internal 8-bit counter on the potentiometer, adjusting its resistance value, and modulating the laser power in turn.

VIII. TESTING

Our optical testing has been completed on the individual optical systems, before integration is possible. Our goal is to perform multiple measurements of pre-prepared samples of PET, styrofoam, and nylon at different concentrations in water to create a database of Raman spectra once integration of the probe optics and the spectrometer is complete.

A. Probe Optics

Testing of the probe optics was performed with an Ocean Optics QE Pro Spectrometer. This device offers a built-in “Raman Mode” with background and laser subtraction for 785 nm. A white light source was utilized for alignment of the system.

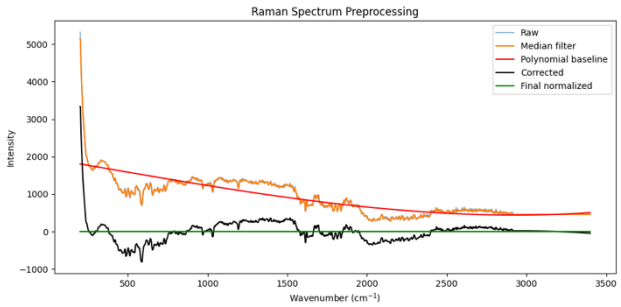

Fig. 5. Styrofoam Spectra Attempt 1. Noisy peaks are visible, but unreliable for detection.

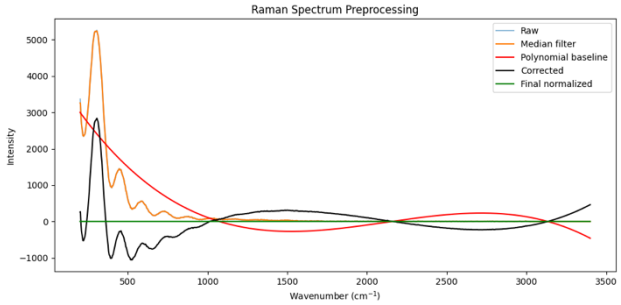

Fig. 6. Styrofoam Spectra Attempt 2. Peaks are visible but follow a suspicious "sinc" like pattern.

The probe optics need further refining. Some consistent peaks are visible in the Styrofoam spectra; however, they are too weak to be reliable for accurate identification. There is also a sinc pattern visible in some of the test attempts. This could be caused by spatial filtering or etaloning between parallel surfaces. Another filter will be added for laser rejection, and slight tilts will be added to the cuvette and intermediary surfaces to minimize coherent interference.

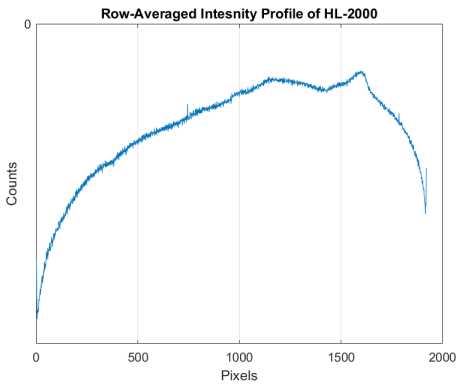

Fig. 7. Broadband spectra taken with our spectrometer using an Ocean Optics HL-2000.

A. *Collection Optics*

System alignment was performed using a white light source to ensure proper beam propagation and component positioning before introducing the 785 nm excitation source. Figure 5 illustrates the broad spectra captured. The curve indicates that there may be some second order present from the diffraction grating hitting the detector as well. Further alignment and focusing is required, along with the use of an order sorting filter.

Various mechanical configurations, including optical posts and 3D-printed housing designs, were explored to provide stable mounting and compact integration of components. We transitioned from optical posts as our mounting system once we got the angles and distances set in stone, to make alignment simpler, and to block out stray light, as shown in Fig. 6.

A. B.

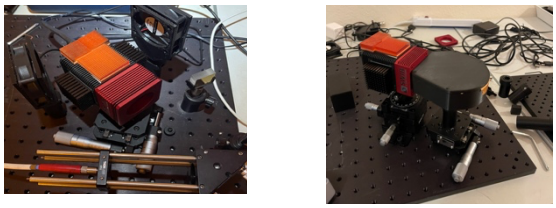

Fig. 8. Figure A displays the previous optical mount system and the new 3D printed enclosure that prevents stray light.

System performance was evaluated through resolution testing using a 785 nm laser to verify spectral accuracy and overall optical alignment. We chose to test with a laser due to its narrow linewidth, and after averaging 10 trials, a FWHM of 1.625 pixels was measured. Based on the dispersion, this can be converted to 0.273 nm, demonstrating a FWHM of 4.44 wavenumbers at the 785 nm excitation wavelengths.

C. Software

Testing of the various software components of ECOspec have primarily been handled in controlled environments, where each system is tested in isolation. Many of these isolated testing environments are enabled through implemented functionality backdoors and debug modes. These techniques provide direct access to specific portions of the software control flow, enabling precise usage for the purpose of system testing.

For testing the primary user interface, alternate functionalities are provided to test primary user-facing elements, such as spectra display. Additionally, hardware

detection methods have been tested using external developer boards to guarantee functionality.

Along with the debug functionality of the UI, testing of the data processing and identification pipeline is provided. Primary testing of these pipelines was performed on data obtained from controlled environments. These test runs validated the design of the processing pipeline, as well as offered guidance for parameter adjustments worth considering. Testing of the identification pipeline was also tested on this sample data and provided results that supported the overall design of the algorithm but showed that accuracy could be increased through refinement and iteration.

Test of the ESP32 control system is still required on version 2 of the PCBs. The test platform was constructed on a breadboard parallel in design to the actual PCB being utilized. With this testbench, manual control of the ESP32 via direct UART commands sent from a host computer enabled control of specific modules, as well as testing the overall communication structure. Subsystems such as servo control, audio output, and laser enable signals all worked as designed, aligning with expectations. Other peripheral systems, such as the digital potentiometer control, require more refinement to ensure precise modulation control and therefore guarantee a safer system for the user.

IX. Conclusion

ECOspec lays the groundwork for a less expensive opto-electric solution for microplastic detection for labs, water quality treatment facilities, and even household use, and has the potential to not only help to solve an environmental concern, but a human health crisis. Microplastics are now present in drinking water, food sources, and the human body, yet detection remains limited and inconsistent. By enabling faster, non-destructive, and more scalable identification of microplastics, ECOspec has the potential to support better regulatory practices, improve environmental monitoring, and increase public awareness of contamination levels. This product is a step towards democratizing chemical analysis tools, bridging the gap between high-end laboratory instrumentation and a practical, deployable solution. With further development, ECOspec could evolve into a portable or networked sensing platform, contributing to large-scale data collection and long-term monitoring efforts. In doing so, it not only supports efforts to mitigate an environmental crisis but also plays a role in protecting human health through improved detection, prevention, and understanding of microplastic exposure.

X. Acknowledgements

We would like to thank Ocean Optics for their continued support and mentorship during both semesters of senior design.

XI. References

[1] H. Ritchie, M. Roser, and V. Samborska, “Plastic Pollution,” Our World in Data, 2023. https://ourworldindata.org/plastic-pollution 2024, doi: https://doi.org/10.1016/j.envres.2024.118535.

[2] S. Ullah et al., “A review of the endocrine disrupting effects of micro and nano plastic and their associated chemicals in mammals,” Frontiers in Endocrinology, vol. 13, Jan. 2023, doi: https://doi.org/10.3389/fendo.2022.1084236.

[3] Y. Lee, J. Cho, J. Sohn, and C. Kim, “Health Effects of Microplastic exposures: Current Issues and Perspectives in South Korea,” Yonsei Medical Journal, vol. 64, no. 5, pp. 301–308, Apr. 2023, doi: https://doi.org/10.3349/ymj.2023.0048.

[4] HORIBA Scientific, “What is raman spectroscopy? - HORIBA,” www.horiba.com. https://www.horiba.com/usa/scientific/technologies/raman-imaging-and-spectroscopy/raman-spectroscopy/

[5] E. S. Jung et al., “Quantitative Raman analysis of microplastics in water using peak area ratios for concentration determination,” npj Clean Water, vol. 7, no. 1, Oct. 2024, doi: https://doi.org/10.1038/s41545-024-00397-4.

[6] I. Chakraborty, S. Banik, R. Biswas, T. Yamamoto, H. Noothalapati, and N. Mazumder, “Raman Spectroscopy for Microplastic Detection in Water sources: a Systematic Review,” International Journal of Environmental Science and Technology, vol. 20, Sep. 2022, doi: https://doi.org/10.1007/s13762-022-04505-0.